ADVANCED FUNCTIONAL MATERIALS
www.afm-journal.de

Light-modulated TiO_x Interlayer Dipole and Contact Activation in Organic Solar Cell Cathodes

*Antonio Guerrero, Sylvain Chambon, Lionel Hirsch, and Germà Garcia-Belmonte**

Understanding working mechanisms of selective interfacial layers and the underlying energetics of the organic semiconductor/electrode interface is an issue of primary concern for improving organic solar cell technologies. TiO_x interlayers are used here to tune the selectivity of the cathode contact to electrons by controlled UV-light activation. The *S*-shaped kink observed for deactivated titania interlayers completely disappears after 2 min of UV-light exposure yielding high fill factor (≈60%) and adequate efficiencies. UV-light activation of complete cells alters the work function of the oxide that decreases about 650 mV as observed by Kelvin probe measurements. Capacitive techniques reveals a light-intensity dependent shift in flat-band voltage of up to 1.2 V under 1 sun illumination (without UV) in the case of deactivated TiO_x interlayers. An increase in the magnitude of the light-modulated dipole present at the oxide layer accounts for that voltage shift. Although the sign of the interface dipole would favor the extraction of electrons, the concomitant modification of the band bending in the organic semiconductor hinders an efficient extraction of carriers at positive voltages and originates the *S*-shaped characteristics. After contact activation, the dipole strength does not change with the light intensity.

1. Introduction

In the last decade, organic photovoltaics (OPV) has become an attractive technology able to replace more expensive and less versatile solar cells. OPV offers the opportunity to use solution process deposition methods known to be compatible with inexpensive fabrication techniques (i.e., inkjet printing or roll to roll). On the other hand, efficiencies have increased steeply in the recent years, that is, up to 10% in the laboratory scale have been obtained, which is regarded as a landmark towards commercialization. To this date degradation of the photovoltaic properties is the main factor that hinders its global implementation. One additional challenge facing this technology is related to the scale up process as it has been observed that the use of mass production printing techniques dramatically reduces the efficiency of the devices. For example a detrimental inflexion point (*S*-shape) in the current density-voltage (*J*–*V*) curves has been observed which destroys the device operation, particularly the fill factor.[1,2] It is recognized that bridging the gap between lab scale and industrial scale solar cell performance relies upon the perfect understanding (from materials to interfaces) of the OPV working principles.

Much data is available regarding the requirements of the materials comprising the organic active layer.[3–5] In a bulk-heterojunction (BHJ) solar cell a polymer donor and fullerene acceptor form a bicontinuous interpenetrated matrix where charge separation and transport of carriers towards the electrodes are enabled. The device works thanks to the presence of selective contacts at either side that can collect electrons and holes at their respective outer electrodes. The role of the highly selective contact is key as must be selective to one carrier while completely blocking the opposite. Interlayers selective to holes include conductive polymers such as poly(3,4-ethylenedioxythiophene):poly(styrenesulfonate)(PEDOT:PSS)[6] and several transition metal oxides (e.g., V_2O_5, MoO_3, NiO, or WO_3).[7–12] Alternatively, interfacial layers selective to electrons include alkali metal compounds as LiF, other metal oxides (TiO_x, ZnO...), or low-molecular weight organic compounds (e.g., BCP).[10,13,14] Among the different approaches to gain carrier selectivity self-assembled monolayers (SAM) or conjugated polyelectrolyte interlayers can be used to alter energy level alignment between the cathode metal and the bulk of the blend.[15,16] It is recognized that electrostatic mechanisms occurring at the interfaces have a great influence on the overall device operation.[17–23] However, the light-induced electrical mechanisms at the contact in relation with the interaction with the bulk properties of the active layer is a terrain that has been much less studied.

TiO_x has been widely used by many authors as an effective interlayer selective to electrons.[24,25] Unfortunately, this material requires UV-light soaking for activation in order to avoid *S*-shaped kink in the *J*–*V* curves under illumination.[26–28] It has been proposed that bandgap shallow charge carrier traps are present in titania, which are filled upon UV irradiation, thereby lowering its series resistance and enhancing photoconductivity.[29,30] Other authors suggested explanations that involve

Dr. A. Guerrero, Prof. G. Garcia-Belmonte
Photovoltaics and Optoelectronic Devices Group
Departament de Física
Universitat Jaume I
12071, Castelló, Spain
E-mail: garciag@fca.uji.es
Dr. S. Sylvain, Prof. L. Hirsch
Univ. Bordeaux
IMS, UMR 5218, F-33400 Talence
France and CNRS, IMS, UMR 5218
F-33400, Talence, France

DOI: 10.1002/adfm.201401233

the interaction with molecular oxygen.[28] However, exact activation mechanism is still unclear. Recently, by carefully selecting the synthetic method, the activated form of TiO_x can be retained during several days.[30] These titania interlayers offer a unique opportunity as TiO_x can be activated/deactivated on demand. By carefully controlling the light soaking process TiO_x interlayer activation can be stopped at different levels. This procedure renders the contact/active layer interface at different energetic states which allows studying the energy level alignment at the cathode contacts in detail by means of electrical techniques.

By using capacitance–voltage measurements a complete picture of the energetics at cathode interfaces is drawn in this work. Here interfacial properties are responsible for the observed photovoltaic parameters. We observe that deactivated TiO_x interlayers show a strong light-dependent interface dipole that increases dramatically up to 1.2 eV under 1 sun irradiation. The dipole layer induces a change in the band bending sign at the active layer blend from electron extracting to electron blocking, which is behind the *S*-shaped *J*–*V* curves. Although the sign of the dipole would favour the extraction of electrons the concomitant modification of the band bending in the organic semiconductor hinders an efficient extraction of carriers. Activated TiO_x interlayers do not produce *S* kink features and consequently high fill factors (≈60%) are observed. The devices studied here represent a unique opportunity of analyzing light-induced effects on outer interfaces. This work provides insights on the contact operation for optimum device engineering which can be applied to other contact structures.

2. Results and Discussion

2.1. Interlayer Activation and Current Density–Voltage Curves

Solar cells have been fabricated using the following inverted architecture Glass/ITO/TiO_x/P3HT:PCBM/MoO_3/Ag as described in the Experimental section. Activation of TiO_x electron selective layer by UV light was promoted by using the xenon lamp of the solar simulator and this activation occurs as previously reported for other light sources (**Figure 1**).[30] *J*–*V* curves at different activation times were measured using the same solar simulator coupled with a UV light filter (400 nm cutoff) (Figure 1a). As reported previously *S*-shaped kinks are observed when TiO_x has not been activated leading to poor device performances (see **Table 1**). *S*-shape evolves with the activation time, and after 2 min the *S* kink is no present any longer. After UV-light activation when no UV filter is used the power conversion efficiencies are in the order of 4.13% (J_{sc} = 12.97 mA cm^{-2}, V_{oc} = 0.530 V, and FF = 60%). Moreover, under dark conditions (Figure 1b) the device behaves as a pure resistor when no activation has taken place, and a rectifying behavior becomes apparent upon activation by UV light.

2.2. Capacitance–Voltage Measurements: Mott-Schottky Analysis

We have previously reported on the energy level equilibration at the active layer/electrode interface accounting for the energy

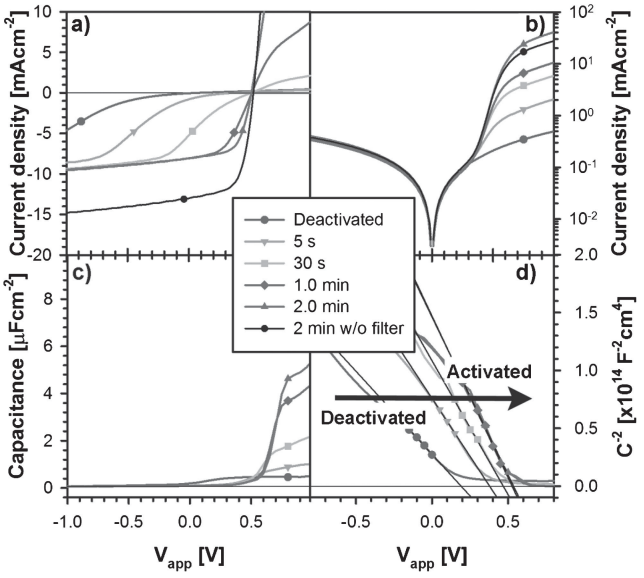

Figure 1. Electrical response of the device as a function of the UV-light activation time. a) Measurements at 1 sun light illumination and b) under dark conditions. c) Capacitance–voltage response and d) Mott-Schottky plots under dark conditions.

mismatch between the workfunction of the cathode Φ_c and the Fermi level of the organic layer E_F.[31] This equilibration takes place by generation of an interface dipole (with strength Δ) being the remaining energy offset accommodated as a band bending in the organic layer. This approach assumes that the anode forms an ohmic contact with the active blend, in such a way that the energy equilibration basically occurs at the cathode. Capacitance-voltage measurements have proved very useful at discerning between active layer band bending and dipole formation.[32] In this technique a DC voltage is applied on working devices, while a small AC perturbation (typically at 100 Hz–1 kHz) is overimposed. The differential displacement current is measured, and the DC voltage is swept over a wide range, that is, −1 V to +1 V. In OPV devices the capacitance is usually flat at negative bias and increases as attainable V_{oc} under illumination is approached (see Figure 1c). At low frequencies the capacitance response is related to the width of the depletion zone at the vicinity of the cathode. By examining Mott-Schottky plots $C^{-2}(V)$ in Figure 1d one can observe straight lines originated by the voltage-modulation of the depletion-zone width.[33] Charge-depleted zones appear as a consequence of the polymer doping

Table 1. Photovoltaic parameters of TiO_x based organic solar cells at different UV-light activation time.

Activation time [s]	J_{sc} [mA cm^{-2}]	V_{oc} [V]	FF [%]	PCE [%]
0	0.06	0.077	23.8	0.00
5	0.83	0.347	17.0	0.05
30	5.17	0.517	17.7	0.47
60	8.04	0.517	47.5	1.97
120	8.04	0.510	60.1	2.47
120 (w/o filter)	12.97	0.530	60.0	4.13

Table 2. Parameters extracted from Mott-Schottky analysis. Doping density N calculated from the Mott-Schottky plot, and flat-band voltage V_{fb}. Dipole calculations include interlayer work function E_{FTiOx} = 4.0 or 4.65 eV, activated and not activated respectively, and active layer Fermi level E_F = 4.9 eV.

UV Light Exposure [s]	Light intensity [Wm^{-2}]	N [$\times 10^{17}$ cm^{-3}]	V_{fb} [V]	Δ [eV]
0	Dark	3.2	0.26	0.00
5	Dark	2.0	0.42	0.16
30	Dark	1.8	0.51	0.40
60	Dark	1.6	0.54	0.36
120	Dark	1.7	0.56	0.38
120	Dark	2.1	0.55	0.35
120	1000	3.5	0.56	0.35
0	Dark	3.5	0.26	0.00
0	50	2.8	0.054	0.20
0	80	2.4	–0.36	0.61
0	250	2.7	–0.46	0.71
0	400	3.2	–0.66	0.90
0	1000	3.0	–0.94	1.19

which can be calculated from the slope of the straight line. Measurable electrical defects arise from external agents such as oxygen traces,[34] residual solvent or intrinsic impurities connected with the domain size of the P3HT.[35] On the other hand, the intercept of the straight line signals the flat band potential V_{fb}, defined as the applied voltage bias required to produce flat bands in the organic semiconductor. The value of V_{fb} is related to the contact energetics by means of the next expression[31]

$$qV_{fb} = E_F - \phi_c - \Delta \quad (1)$$

Equation 1 is easily viewed when $V_{app} = V_{fb}$ as explained later. Here it is assumed that the electrode contact Fermi level (workfunction of the cathode ϕ_c) equals the TiO_x interlayer Fermi level E_{FTiOx}.[31] The dipole is formed because the TiO_x interlayer is negatively charged and compensated by positive charge located at the electrode side. For a given system a shift in the measured V_{fb} may be related to any of the three parameters in the right side of Equation 1, and understanding its origin provides key information. For example, recently we have been able to correlate shifts in V_{fb} with variations in fullerene composition at the organic layer/cathode interface, which modulates the amplitude of the interface dipole.[32]

Regarding devices fabricated with TiO_x interlayers activated under different UV light exposure times, Mott-Schottky plots under dark conditions show a shift in the flat band potential of about 300 mV towards more positive voltages for activated devices (Figure 1d and **Table 2**). V_{fb} of activated samples is very similar to those obtained with other contacts such as Ca or Al.[31] This fact suggests that the Fermi level of the organic semiconductor should remain constant upon UV exposure, being the interlayer Fermi level E_{FTiOx} shifted to an upper position. This process can be regarded as a sort of UV-light photodoping of the TiO_x interlayer. We will discuss latter on the energetics of the activation mechanism.

Additionally, C–V measurements as a function of the light intensity have been carried out. When an activated device is illuminated the position of the flat band potential does not change significantly (**Figure 2**b). Both E_{FTiOx} and Δ remain unaltered. However, if a deactivated device is measured under different illumination intensities (w/o UV), the V_{fb} shifts strongly. Indeed, when measurements under dark conditions and those at 1 sun light intensity are compared a shift of over 1.2 V occurs (Figure 2d). Moreover V_{fb} attains even negative values indicating a change in the band bending sign. It occurs that V_{fb} shifts depending on whether titania has been activated or not, and this effect is pronounced for deactivated devices under illumination. As this is an intrinsic effect of the TiO_x

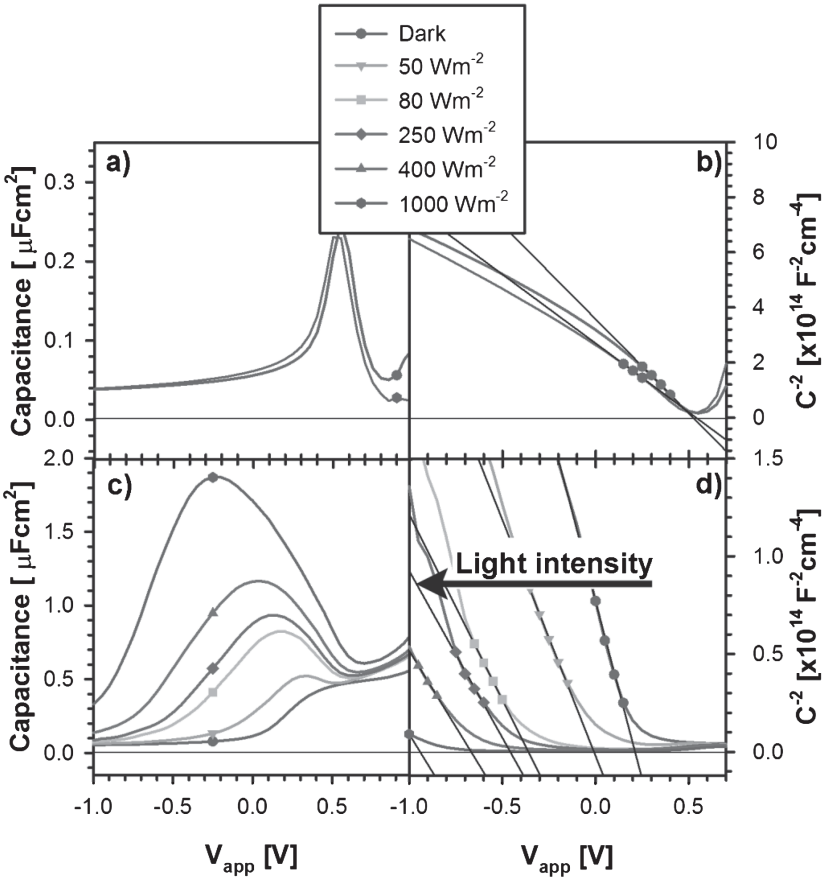

Figure 2. a,b) Capacitance–voltage measurements of an activated device under dark and 1 sun light intensity conditions. c,d) Capacitance–voltage measurements of a device that has not been UV-light activated as a function of the light intensity.

interlayer one can exclude a modification in the active layer E_F position. This would imply that it is the alteration of the dipole height Δ that lies behind the V_{fb} shifts of deactivated samples. In summary it is proposed that UV-light exposure modifies the TiO_x interlayer work function E_{FTiOx}, while white-light irradiation of deactivated cells induces a change in the dipole strength Δ according to Equation 1.

2.3. Energy Band Profile for Deactivated TiO_x

Considering the large negative shift in V_{fb} observed after illumination in Figure 2d, an energy diagram as that shown in **Figure 3** reproduces the energetic band profile of a device comprising a deactivated TiO_x interlayer. Under dark conditions and at $V_{app} = 0$ V (Figure3a) band bending would favour the extraction of electrons at the cathode, while a relatively small dipole is present. In the dark a positive applied bias is required to attain flat bands in the organic semiconductor. If the device is illuminated using low intensities, i.e. 50 Wm^{-2}, the photogenerated electrons coming from the active layer accumulate at the TiO_x interface increasing the dipole strength (Figure3b). The energy mismatch between TiO_x and active layer is reduced thanks to the presence of a larger dipole, and the band bending consequently decreases. The required potential to have flat bands will be smaller than under dark conditions. Since the electrical field in the organic side of the selective layer is decreased the extraction of electrons is reduced in comparison to the dark case. Upon further increase of the irradiation intensity, the accumulated charge density at the TiO_x interlayer increases. It then modifies the energetic levels in the bulk of the active layer. Under high illumination conditions (Figure 3c) bands in the organic semiconductors are inverted and would facilitate the extraction of holes across the cathode, then impeding a correct operation of the solar cell. In this last case flat bands are attained at negative bias values. Intuitively one might expect that having a larger dipole with the correct sign should favor the extraction of carriers, however, this does not occur as the energetic profile at the organic semiconductor changes sign. As TiO_x workfunction does not change upon illumination without UV (see Kelvin probe experiments in Supporting Information), the large shift of 1.2 V observed in V_{fb} during UV-filtered white-light illumination of the deactivated device cannot be related to a modification of the workfunction of TiO_x, and must be originated by the change in magnitude of a dipole that opposes the efficient extraction of carriers.

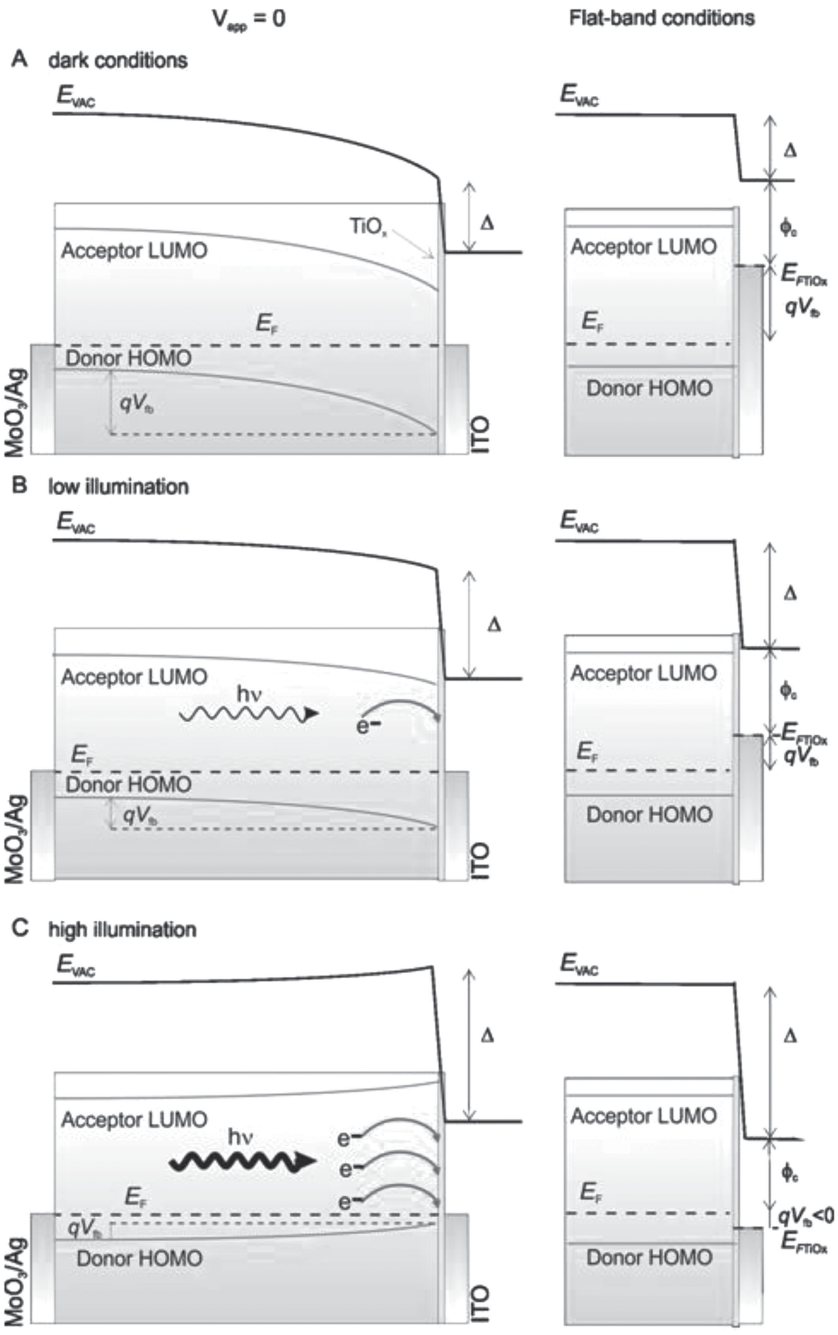

Figure 3. Energy level diagram of a device containing TiO_x deactivated layer that a) under dark conditions, b) low illumination, and c) high illumination. The dipole increases with the light intensity. The degree and sign of the band bending under equilibrium conditions are therefore modified with the white-light intensity. There is a clear shift in V_{fb} indicating that the magnitude of the dipole increases with the light intensity. The band bending is reversed hindering an efficient extraction of electrons.

The previous scheme explains the observed *S*-shaped kink in the *J*–*V* characteristics of Figure 1a. Light irradiation promotes electrons to accumulate at the TiO_x interface, changing as a consequence the dipole strength and the active layer

band bending. A detailed analytical model accounting for the observed both *J–V* and *C–V* curves was proposed by Bisquert et al.[36] The model stressed the role of the occupancy of interlayer states (mediating charge transfer across the contact) as a function of bias or illumination.

To gain further insight into the device operation, impedance spectroscopy measurements were performed on samples activated over different exposure times by UV light, and these results are shown and discussed as Supporting Information. For deactivated sample an additional resistance and capacitance is observed at low frequencies indicating the presence of charge accumulation at the TiO_x layer. Interestingly, it appears that each of the voltage dependence of capacitive and resistive responses are shifted with the UV light exposure time. Indeed, if the voltage axis is displaced using the value of the dipole calculated in Table 2 (see below), the different responses collapse. The implications of this observation are very important as this entails that once the energy offset of the dipole has been overcome by applying an external voltage, the carrier density and recombination properties in the active layer become very similar independently of the activation degree.

2.4. Origin of UV Light Activation of TiO_x

Activation of TiO_x interlayer by UV light is not totally understood and is still under discussion. Whilst Schmidt et al.[28] suggested that activation is related to adsorbed molecular oxygen, Kim et al.[27] supported that shallow charge carrier traps are present in the bandgap of TiO_x, being responsible for the *S*-shaped *J–V* curves. In this second case traps may be filled upon UV irradiation of the TiO_x interlayer therefore improving its series resistance and photoconductivity.[30] In order to further understand this effect, Kelvin probe (KP) measurements have been carried out aiming at determining the titania interlayer work function variation under UV light exposure. **Figure 4** shows a representative KP measurement on substrates with the configuration Glass/ITO/TiO_x where the contact potential difference (CPD) is monitored over a period of 4000 s. A freshly evaporated gold layer (100 nm) has been used as a reference. Under dark conditions the work function is stable and after exposing the sample to UV light (365 nm) its value decreases about 650 mV over a period of 3000 s. On the other hand, when the TiO_x layer is illuminated with a green LED (538 nm) no change in the work function is observed (see Supporting Information). The shift in work function with UV exposure agrees with the increment in V_{fb} observed in Figure 1d, although full activation is attained much faster in devices because of the use of intense UV source. This is qualitative indication that a displacement of the TiO_x interlayer Fermi level E_{FTiOx} is the responsible for the V_{fb} offset upon UV light exposure. Once the light is switched off the work function slowly recovers its original value.

TiO_x work function values for deactivated (4.65 eV), and full activated (4.0 eV) have been calculated from KP measurements using a reference gold specimen (considering gold work function at 4.8 eV). This change qualitative agrees with the shift in the flat band potential of about 300 mV towards negative values for deactivated devices (see Figure 1d). Nonetheless it should be stressed that changes in the titania work function can also occur after deposition of the organic layer. The dipole strength Δ is then calculated using Equation 1, and its values are summarized in Table 2. Here the active layer Fermi level $E_F \approx 4.9$ eV is estimated from the doping density *N* in Table 2 and the polymer HOMO position ($E_{HOMO} = 5.0$ eV). It is interesting to note that Δ is not present in dark conditions using deactivated samples. The contact equilibration is assured by the active layer band bending. Δ value increases as a function of the white-light intensity that completely accounts for the negative shift in V_{fb}. The contact energetics changes radically for activated samples. In this last case the dipole strength is not modulated by the light intensity exhibiting similar values in the dark and under 1 sun irradiation.

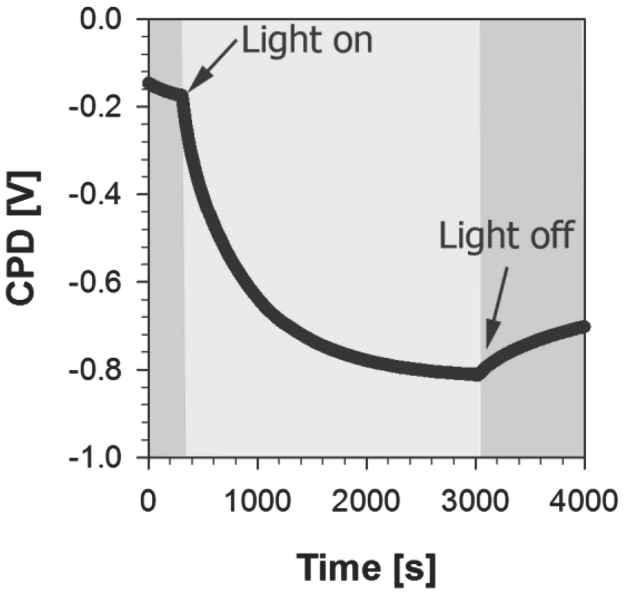

Figure 4. Kelvin probe measurement under dark and after exposure to UV light (365 nm). The contact potential difference (CPD) is monitored over a period of 4000 s. A freshly evaporated gold layer (100 nm) has been used as a reference.

Figure 5a sketches the origin of the dipole strength change in relation to the presence of interface sites. For deactivated

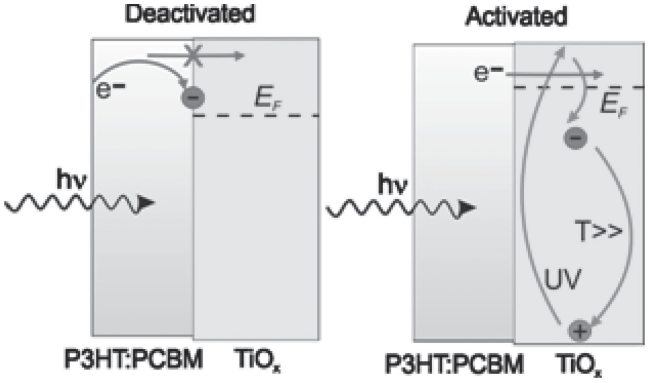

Figure 5. a) Charge built-up at TiO_x interface after illumination in its deactivated form, and blocking of the electron extraction. b) Activation and deactivation process of the TiO_x interlayer by the action of UV light and temperature, respectively.

TiO_x, once the active layer is illuminated with white light (with UV filter) photogenerated electrons accumulate at the organic layer/metal oxide interface. Electrons cannot go through the TiO_x due to its very low conductivity before activation.[30] This process piles up negative charge at the TiO_x interlayer, and enlarges the magnitude of the dipole. At a given white-light irradiation electron accumulation stops by the formation of reverse bandbending. In the extreme case when 1 sun light illumination is used a shift of up to 1.2 eV in the dipole is observed. This interfacial mechanism is highly reversible and the dipole height is rapidly reduced upon light switch-off. Alternatively, when the TiO_x is illuminated with UV light electrons are promoted from the valence band to the trap states (Figure 5b). UV-light induced charge modifies both E_{FTiOx} and Δ, presumably because processes occur either in the TiO_x bulk traps (E_{FTiOx}) or interface sites (Δ). In other words, a capacitor is formed with the deactivated TiO_x as dielectric, which is polarized under UV-filtered white light illumination. In case of activated TiO_x, its work function is reduced and this layer becomes more conductive assisting then electron collection. Deactivation of the TiO_x may be induced by a thermal treatment where the electrons filling the traps thermalize to the ground state. It is concluded that the activation mechanism inferred here agrees with that proposed previously.[27,30]

3. Conclusion

In this work we have studied the operation mechanism of an interfacial layer selective to electrons, and its relationship with the energetics of the organic semiconductor/electrode interface. We use TiO_x in working devices as a model where the electron selectivity can be tuned by the activation through UV-light exposure. Here we observe that upon full activation of TiO_x the work function of the oxide decreases about 650 meV in complete devices. It is remarkable the increase in the magnitude of the dipole present at the TiO_x/active layer interface, up to 1.2 eV under 1 sun light illumination in deactivated cells. The sign of the dipole would favour the extraction of electrons, however, the concomitant modification of the energy levels in the organic semiconductor hinders an efficient extraction of carriers. After contact activation the dipole strength does not change with the light intensity. This work provides insights on the contact operation for optimum device engineering and modeling.

4. Experimental Section

Solar cells have been fabricated using the following inverted architecture Glass/ITO/TiO_x/P3HT:PCBM/MoO_3/Ag. 15 mm × 15 mm (indium tin oxide) ITO-coated glass sheets (10 Ω/□, Visiontek Systems) are successively cleaned in acetone, ethanol and isopropanol in an ultrasonic bath and exposed to UV-ozone for 15 min. Titanium oxide is prepared as followed: Titanium (IV) isopropoxide (TIPT, Aldrich, 99.999%) is diluted in absolute ethanol at a concentration of 0.05 M, to which HCl is added in order to have a water to TIPT molar ratio (rw) of 0.82 and a pH of 1.9. The precursor solution is stirred for 72 h at room temperature. 40 µL of TiO_x solution is spin coated on the substrate in air (ambient atmosphere) at 1000 rpm for 60 s and kept in air at room temperature for 2 hours. Subsequently the substrates were transferred to a nitrogen-filled glovebox (O_2 and H_20 < 0.1 ppm). Starting from this point, the rest of the fabrication process and all the *J–V* characterizations are carried out under inert atmosphere. TiO_x coated ITO sheets were then thermally treated at 80 °C for 10 min on temperature-controlled hot plate. We choose low annealing temperature as a processing compatible with printed flexible electronics. TiO_x layer thickness was measured to be 20 ± 5 nm using a Tencor IQ profilometer. Poly(3-hexylthiophene) (P3HT, Plexcore OS2100) and 1-(3-methoxycarbonyl) propyl-1-phenyl[6,6]C61 (PCBM, 99.5%) were supplied from Plextronics and Solaris-Chem Inc. respectively and used as received. Solutions were prepared in o-dichlorobenzene, at a 1:1 weight ratio and a concentration of 20 mg mL^{-1}. Solutions were first stirred at 90 °C for 10 min and subsequently at 50 °C for 24 h. P3HT:PCBM was spincoated at 1000 rpm during 50 s. Instantly after spin-coating, the substrates were individually placed in small closed petri dishes overnight at room temperature for solvent annealing. The resulting P3HT:PCBMthickness was 240 ± 10 nm. 10 nm of molybdenum trioxide (MoO_3, Serac) and 80 nm of silver (Ag) were successively thermally-evaporated under a secondary vacuum (10^{-6} mbar) onto the P3HT:PCBM layer through a shadow mask to define a 10 mm^2 active area. Devices were encapsulated using a microscopy slide and epoxy for further electrical characterization outside the glovebox. The devices were characterized using an ATLAS Solarconstant 1200 solar simulator (metal-halide 1200 W lamp) with AM1.5G filters set at 100 mW cm^{-2} with a calibrated radiometer (IL 1400BL). Labview-controlled Keithley 2400 SMU enabled the measurement of current density–voltage (*J–V*) curves. The solar simulator was used to activate the devices during specific times and a UV-filter (400 nm cutoff) was used to characterize the devices under illumination at those different activation times. We would like to emphasize that the light intensity has been measured without filter meaning that the *J–V* characteristics with UV filter are affected by the absorption and reflection of the filter. It is the reason why the short-circuit current (Table 1) with and without filter is different.

The contact potential difference (CPD) of the TiO_x layer was determined using Besocke Delta Phi Kelvin Probe (Kelvin probe S and Kelvin control 07). Gold substrate was used to calibrate the equipment. UV light-emitting diode (LED Engin) emitting at 365 nm was used to illuminate the TiO_x layer during the CPD experiment.

Capacitance–voltage (*C–V*) measurements were performed with an Autolab PGSTAT-30 equipped with a frequency analyzer module, and was recorded by applying a small voltage perturbation (20 mV). Measurements were carried out at different light intensity and bias voltage at a fixed frequency of 1 kHz. A UV light filter with cutoff wavelength of 400 nm (Thorn Labs FGL 400s) was used between light source and sample to avoid undesired TiO_x activation. The light intensity was measured using an optical power meter 70310 from Oriel Instruments where a certified Si photodiode was used to calibrate the system.

Supporting Information

Supporting Information is available from the Wiley Online Library or from the author.

Acknowledgements

The authors thank financial support from Generalitat Valenciana (ISIC/2012/008 Institute of Nanotechnologies for Clean Energies). This work has been financially supported by the French National Research Agency (Agence Nationale de la Recherche) in the frame of the project ANR-13-JS09–0014–01 "IN-STEP" and the French PHC NANO ESPAGNE 2013 project n° 31388XJ.

Received: April 17, 2014
Revised: June 10, 2014
Published online: August 14, 2014

[1] M. R. Lilliedal, A. J. Medford, M. V. Madsen, K. Norrman, F. C. Krebs, *Solar Energy Mater. Solar Cells* **2010**, *94*, 2018.
[2] B. Tremolet de Villers, C. J. Tassone, S. H. Tolbert, B. J. Schwartz, *J. Phys. Chem. C* **2009**, *113*, 18978.
[3] G. Li, V. Shrotriya, J. Huang, Y. Yao, T. Moriarty, K. Emery, Y. Yang, *Nat. Mater.* **2005**, *4*, 864.
[4] X. Yang, J. Loos, S. C. Veenstra, W. J. H. Verhees, M. M. Wienk, J. M. Kroon, M. A. J. Michels, R. A. J. Janssen, *Nano Lett.* **2005**, *5*, 579.
[5] H. Hoppe, N. S. Sariciftci, *J. Mater. Chem.* **2006**, *16*, 45.
[6] G. Greczynski, T. Kugler, M. Keil, W. Osikowicz, M. Fahlman, W. R. Salaneck, *J. Electron Spectrosc. Relat. Phenom.* **2001**, *121*, 1.
[7] S. Schubert, M. Hermenau, J. Meiss, L. Müller-Meskamp, K. Leo, *Adv. Funct. Mater.* **2012**, *22*, 4993.
[8] J. Meyer, S. Hamwi, M. Kroger, W. Kowalsky, T. Riedl, A. Kahn, *Adv. Mater.* **2012**, *24*, 5408.
[9] H.-Q. Wang, N. Li, N. S. Guldal, C. J. Brabec, *Organ. Electron.* **2012**, *13*, 3014.
[10] E. L. Ratcliff, B. Zacher, N. R. Armstrong, *J. Phys. Chem. Lett.* **2011**, *2*, 1337.
[11] T. Ripolles-Sanchis, A. Guerrero, E. Azaceta, R. Tena-Zaera, G. Garcia-Belmonte, *Solar Energy Mater. Solar Cells* **2013**, *117*, 564.
[12] F. Guillain, D. Tsikritzis, G. Skoulatakis, S. Kennou, G. Wantz, L. Vignau, *Solar Energy Mater. Solar Cells* **2014**, *122*, 251.
[13] R. Steim, F. R. Koglera, C. J. Brabec, *J. Mater. Chem.* **2010**, *20*, 2499.
[14] R. Po, C. Carbonera, A. Bernardia, N. Camaioni, *Energy Environ. Sci.* **2011**, *4*, 285.
[15] H.-L. Yip, S. K. Hau, N. S. Baek, H. Ma, A. K. -Y. Jen, *Adv. Mater.* **2008**, *20*, 2376.
[16] J. H. Seo, A. Gutacker, Y. Sun, H. Wu, F. Huang, Y. Cao, U. Scherf, A. J. Heeger, G. C. Bazan, *J. Am. Chem. Soc.* **2011**, *133*, 8416.
[17] D. H. Wang, J. S. Moon, J. Seifter, J. Jo, J. H. Park, O. O. Park, A. J. Heeger, *Nano Lett.* **2011**, *11*, 3163.
[18] B. Schmidt-Hansberg, M. Sanyal, M. F. G. Klein, M. Pfaff, N. Schnabel, S. Jaiser, A. Vorobiev, E. Müller, A. Colsmann, P. Scharfer, D. Gerthsen, U. Lemmer, E. Barrena, W. Schabel, *ACS Nano* **2011**, *5*, 8579.
[19] H. Ishii, K. Sugiyama, E. Ito, K. Seki, *Adv. Mater.* **1999**, *11*, 605.
[20] X. Crispin, V. Geskin, A. Crispin, J. Cornil, R. Lazzaroni, W. R. Salaneck, J.-L. Bredas, *J. Am. Chem. Soc.* **2002**, *124*, 8131.
[21] J. Hwang, A. Wan, A. Kahn, *Mater. Sci. Eng. R Rep.* **2009**, *64*, 1.
[22] S. Braun, W. R. Salaneck, M. Fahlman, *Adv. Mater.* **2009**, *21*, 1450.
[23] (Eds: W. R. Salaneck, K. Seki, A. Kahn, J.-J. Pireaux), *Conjugated Polymer and Molecular Interfaces. Science and Technology for Photonic and Optoelectronic Applications*Marcel Dekker, New York **2002**.
[24] S. H. Park, A. Roy, S. Beaupré, S. Cho, N. Coates, J. S. Moon, D. Moses, M. Leclerc, K. Lee, A. J. Heeger, *Nat. Photonics* **2009**, *3*, 297.
[25] G. Li, R. Zhu, Y. Yang, *Nat. Photonics* **2012**, *6*, 153.
[26] T. Kuwabara, C. Iwata, T. Yamaguchi, K. Takahashi, *ACS Appl. Mater. Interfaces* **2010**, *2*, 2254.
[27] C. S. Kim, S. S. Lee, E. D. Gomez, J. B. Kim, Y.-L. Loo, *Appl. Phys. Lett.* **2009**, 94.
[28] H. Schmidt, K. Zilberberg, S. Schmale, H. Flügge, T. Riedl, W. Kowalsky, *Appl. Phys. Lett.* **2010**, *96*, 243305.
[29] C. S. Kim, S. S. Lee, E. D. Gomez, J. B. Kim, Y.-L. Looa, *Appl. Phys. Lett.* **2009**, *94*, 113302.
[30] S. Chambon, E. Destouesse, B. Pavageau, L. Hirsch, G. Wantz, *J. Appl. Phys.* **2012**, *112*, 094503.
[31] A. Guerrero, L. F. Marchesi, P. P. Boix, S. Ruiz-Raga, T. Ripolles-Sanchis, G. Garcia-Belmonte, J. Bisquert, *ACS Nano* **2012**, *6*, 3453.
[32] A. Guerrero, B. Dörling, T. Ripolles-Sanchis, M. Aghamohammadi, E. Barrena, M. Campoy-Quiles, G. Garcia-Belmonte, *ACS Nano* **2013**, *7*, 4637.
[33] P. P. Boix, G. Garcia-Belmonte, U. Munecas, M. Neophytou, C. Waldauf, R. Pacios, *Appl. Phys. Lett.* **2009**, *95*, 233302.
[34] A. Guerrero, P. P. Boix, L. F. Marchesi, T. Ripolles-Sanchis, E. C. Pereira, G. Garcia-Belmonte, *Solar Energy Mater. Solar Cells* **2012**, *100*, 185.
[35] T. S. Ripolles, A. Guerrero, G. Garcia-Belmonte, *Appl. Phys. Lett.* **2013**, *103*, 243306.
[36] J. Bisquert, G. Garcia-Belmonte, A. Munar, M. Sessolo, A. Soriano, H. J. Bolink, *Chem. Phys. Lett.* **2008**, *465*, 57.